THE JOURNAL OF BIOLOGICAL CHEMISTRY
Vol. 279, No. 28, Issue of July 9, pp. 28961–28969, 2004
Printed in U.S.A.

Saccharomyces cerevisiae Hop1 Zinc Finger Motif Is the Minimal Region Required for Its Function *in Vitro**

Received for publication, April 5, 2004, and in revised form, April 26, 2004
Published, JBC Papers in Press, April 28, 2004, DOI 10.1074/jbc.M403727200

S. Anuradha and K. Muniyappa‡

From the Department of Biochemistry, Indian Institute of Science, Bangalore 560012, India

Saccharomyces cerevisiae **meiosis-specific *HOP1*, which encodes a core component of synaptonemal complex, plays a key role in proper pairing of homologous chromosomes and processing of meiotic DNA double strand breaks. Isolation and analysis of *hop1* mutants indicated that these functions require Cys^{371} of Hop1 embedded in a region (residues 343–378) sharing homology to a zinc finger motif (ZnF). However, the precise biochemical function of Hop1, or its putative ZnF, in these processes is poorly understood. Our previous studies revealed that Hop1 is a DNA-binding protein, showed substantially higher binding affinity for G4 DNA, and enhances its formation. We report herein that ZnF appears to be sufficient for both zinc as well as DNA-binding activities. Molecular modeling studies suggested that Hop1 ZnF differs from the previously characterized natural ZnFs. The zinc-binding assay showed that the affinity for zinc is weaker for C371S ZnF mutant compared with the wild type (WT) ZnF. Analysis of CD spectra indicated that zinc and DNA induce substantial conformational changes in WT ZnF, but not in C371S ZnF mutant. The results from a number of different experimental approaches suggested that the DNA-binding properties of ZnF are similar to those of full-length Hop1 and that interaction with DNA rich in G residues is particularly robust. Significantly, WT ZnF by itself, but not C371S mutant, was able to bind duplex DNA and promote interstitial pairing of DNA double helices via the formation of guanine quartets. Together, these results implicate a direct role for Hop1 in pairing of homologous chromosomes during meiosis.**

For faithful segregation of homologous chromosomes during meiosis I, each chromosome must recognize, pair, and recombine with its correct partner. This is achieved by a string of rather poorly defined processes. However, it has become increasingly apparent that, prior to segregation, homologous chromosomes undergo a series of biochemical changes that increase their compaction (1), reorganize their orientation in the nucleus (reviewed in Ref. 2), and resolve spatial and topological issues among and within themselves (3–5). In many eukaryotes, pairing culminates in synapsis, wherein homologous chromosomes are physically linked along their entire lengths by a meiosis-specific proteinaceous structure called the synaptonemal complex (SC)[1] (reviewed in Ref. 3). Several lines of evidence indicate that genetic exchange between homologous chromosomes occurs in this context, which is facilitated by the formation of chiasmata (6). Ultrastructural analysis reveals that the SC is composed of two lateral elements, one on each homologue, and a central element that, in turn, are linked by transverse elements (7, 8).

The precise mechanism by which the SC components facilitate pairing of meiotic chromosomes is unclear. However, observations of presynaptic alignment and the display of substantial levels of homologue pairing in asynaptic organisms implicate a role for SC in maintaining rather than initiating pairing of homologues (reviewed in Ref. 7). In addition, homologous chromosomes interact with each other during genetic exchange in the absence of SC. These interactions are not prerequisites for pairing; rather, they are believed to contribute to the maintenance of pairing. Consistent with these observations, numerous yeast mutants that are deficient in homologous recombination do not completely lack pairing, although the amount of pairing is decreased and synapsis is defective in these mutants (9–11).

In *Saccharomyces cerevisiae*, genetic analyses have identified mutants defective in meiotic chromosome synapsis, some of which produce strong asynaptic phenotypes and abnormal SC structures (7, 8). The genes that encode SC components include *HOP1*, *HOP2*, *RED1*, *ZIP1*, *ZIP2*, and *ZIP3* (12–19). *HOP1*, which specifies a component of lateral element of SC, is required for proper pairing of meiotic chromosomes (13), whereas the *HOP2* gene product quells synapsis between non-homologous chromosomes (19). Like Hop1, Red1 is a major component of SC lateral elements (20). Hop1 colocalizes with Red1 to discrete sites on axial elements, which serve as precursors to lateral elements; however, Hop1 dissociates as these elements become incorporated into mature SCs (20). The Zip1 protein localizes along the lengths of synapsed meiotic chromosomes and serves as a major component of the central regions of SC (16). Zip2 and Zip3 are present on meiotic chromosomes at discrete foci that correspond to the sites where synapsis initiates, and these proteins are required for the proper assembly of Zip1 along meiotic chromosomes (18). However, the mechanisms underlying the functions of any of the SC proteins in chromosome pairing has not been established. In this regard, we reported that Hop1 protein is a structure-specific DNA-binding protein (21) and that it is capable of promoting synapsis between a pair of double-stranded DNA helices (22). Importantly, the interaction between double-stranded DNA helices occurs in a G4 DNA-dependent manner (22). These studies

* This work was supported by a grant from the Department of Science and Technology, New Delhi. The costs of publication of this article were defrayed in part by the payment of page charges. This article must therefore be hereby marked "*advertisement*" in accordance with 18 U.S.C. Section 1734 solely to indicate this fact.

‡ To whom correspondence should be addressed. Tel.: 91-80-2394-2235/2360-0278; Fax: 91-80-2360-0814/0683; E-mail: kmbc@biochem.iisc.ernet.in.

[1] The abbreviations used are: SC, synaptonemal complex; BSA, bovine serum albumin; CD, circular dichroism; DTT, dithiothreitol; form I DNA, negatively supercoiled DNA; form II DNA, nicked circular double-stranded DNA; form III DNA, linear double-stranded DNA; WT, wild-type; ZnF, zinc-finger motif; FBA, filter binding assay.

revealed a biochemical function for Hop1, first for any SC component, in interstitial pairing of meiotic chromosomes.

Zinc fingers (ZnF) are among the most ubiquitous protein domains found in eukaryotic organisms. The variant forms of ZnFs are distinguished by the arrangement of conserved zinc binding ligands: the most common configurations are CCHH, CCCC, CCHC, or CHCC motifs. The Cys_2/His_2 ZnFs fold into $\beta\beta\alpha$ structure by Zn^{2+} binding. The ZnF structure is stabilized by Zn^{2+} coordination of conserved histidine and cysteine residues and hydrophobic interaction among other residues in the ZnF. ZnFs function as recognition elements for interaction with DNA, RNA, or other proteins with high affinity (reviewed in Ref. 23). Sequence comparisons previously identified a motif ($^{348}CX_2CX_{19}CX_2C^{374}$) (hereafter referred to as ZnF motif) in Hop1 (13, 24), reminiscent of the Cys_2/Cys_2 type ZnF found in eukaryotic transcription factors (25). The Cys_2/Cys_2 motif of Hop1 appears to be crucial for its function in meiosis, because a single mutation of C371S within the putative ZnF renders the *hop1* mutant allele defective in sporulation and meiosis (13, 24). Because ZnFs are often sequence-specific DNA-binding motifs, we asked whether Hop1 ZnF might bind DNA in a specific fashion. In this study, we have taken a biochemical approach to delineate the role of putative ZnF implicated in Hop1 function. Intriguingly, we find that Hop1 ZnF displays all of the known activities of full-length Hop1 protein. Together, these results implicate a direct role for Hop1 in meiotic chromosome pairing, processing of meiotic double-strand breaks, and recombination.

MATERIALS AND METHODS

Peptides, DNA, and Enzymes—The wild type Hop1-putative ZnF and its corresponding mutant peptide were obtained from Genemed Synthesis, Inc. The peptides were dissolved in buffer containing 10 mM Tris-HCl (pH 7.5) and 1 mM DTT, and their concentrations were determined at $A_{275\ nm}$ (ϵ_{275} of Tyr = 1420 M^{-1} cm^{-1} and ϵ_{275} of Cys = 145 M^{-1} cm^{-1}). The oligonucleotides were procured from Microsynth, Switzerland. Their sequences are as follows: 4G3, AATTCTGGGTGTGTGGGTGTGTGGGTGTGTGGGTGTGG; 6G3, AATTCTGGGTGTGTGGGTGTGTGGGTGTGTGGGTGTGTGGGTGTGTGGGTGTGG; OX-1T, ACTGTCGTACTTGATATTTTGGGGTTTTGGGGAATGTGA. T4 polynucleotide kinase was obtained from Invitrogen. The oligonucleotides or the top strand of the duplex DNA was labeled at the 5′-end using [γ-^{32}P]ATP and T4 polynucleotide kinase (26). Free ATP was removed by gel filtration using a Sephadex G50 column (26). The labeled strand of each duplex was annealed with an equimolar amount of unlabeled complementary strand. The annealing mixture was electrophoresed on a 6% non-denaturing polyacrylamide gel in 89 mM Tris borate buffer (pH 8.3) containing 1 mM EDTA. Duplex DNA was excised from the gel, eluted into TE buffer (10 mM Tris-HCl, pH 7.5, 1 mM EDTA), and precipitated with 0.3 M sodium acetate (pH 5.2) and 3 volumes of 95% ethanol. The pellet was washed with 70% ethanol, dried, and resuspended in a minimum volume of TE buffer. G4 DNA using 4G3 and OX-1T oligonucleotides were prepared and isolated as described previously (21). Circular single-stranded DNA and negatively superhelical DNA (form I) were prepared from bacteriophage M13 as described previously (27). Linear DNA (form III) was prepared by cleaving M13 form I DNA with BamHI as specified by the manufacturer.

Radioactive Zinc Blotting Assay—Increasing concentrations of WT Hop1 ZnF or its corresponding C371S mutant peptide were vacuum-blotted onto a nitrocellulose filter strip, which was presoaked in buffer A (10 mM Tris-HCl, pH 7.5, 0.3 M NaCl, 10 mM EDTA, and 2 mM DTT). The blot was then incubated at 37 °C for 1 h followed by three washes of 15 min each with binding buffer B (10 mM Tris-HCl, pH 7.5, 0.3 M NaCl). Subsequently, it was incubated with 40 μCi of $^{65}ZnCl_2$ (specific activity, 138.66 mCi/g, Bhabha Atomic Research Center, Mumbai, India) in buffer B for 1 h at 24 °C. The unbound ^{65}Zn was removed by washing the membrane three times with buffer B for 20 min. In the competition experiments, the indicated concentrations of metal ions were present in the buffer during all steps. The blot was then dried and visualized by autoradiography. The bands were quantified using the UVItech gel documentation system with UVI-BANDMAP software, and the values obtained were plotted using Graph pad Prism software.

Electrophoretic Mobility Shift Assays—Reaction mixtures (20 μl) contained 20 mM Tris-HCl, pH 7.5, 0.1 mM $ZnCl_2$ and indicated concentrations of ^{32}P-labeled DNA (duplex or single-stranded or G4 DNA) and Hop1 WT or mutant peptide. Samples were incubated at 30 °C for 30 min and analyzed as described previously (28). Samples were electrophoresed on either 0.8% agarose or 8% polyacrylamide gels at 4 °C in 45 mM Tris borate buffer (pH 8.3) containing 1 mM EDTA at 10 V/cm for 4 h. DNA-binding reactions with G4 DNA were analyzed as described (21). Assays for G4 DNA formation were performed as described (21). Briefly, increasing concentrations of Hop1 WT or mutant peptides were incubated with ^{32}P-labeled oligonucleotide (48-mer) and analyzed as described (21).

Nitrocellulose Filter Binding Assays—Nitrocellulose filters (0.45 μm; Sartorius) were treated with 0.5 M KOH for 30 min at 4 °C and washed extensively with filter binding assay (FBA) buffer (20 mM Tris-HCl, pH 7.5, and 50 mM NaCl) prior to use. Increasing concentrations of the Hop1 WT or mutant peptide and the indicated DNA substrate were mixed in 20 μl of buffer (20 mM Tris-HCl, pH 7.5, and 0.1 mM $ZnCl_2$). After incubation at 30 °C for 30 min, a 10-μl aliquot was applied onto a nitrocellulose filter (for determination of total radioactivity), and the remaining 10 μl was diluted into 0.8 ml of cold FBA buffer. The diluted samples were applied onto KOH-treated filters under vacuum and immediately washed with 5 ml of cold FBA buffer. The filters were dried, and the bound radioactivity was quantified by liquid scintillation. The data were analyzed by non-linear regression equation using the GraphPad Prism software. The peptide concentration at half-maximal binding yielded the apparent dissociation constant (K_d) for various DNA substrates.

Circular Dichroism Measurements—All the CD measurements were made on a Jasco J-715 spectropolarimeter with constant nitrogen purge. CD spectra were recorded at 25 °C in a 2-mm path length cell with a resolution of 0.2 nm over the wavelength range of 200–250 nm. Each spectrum represented the average of two scans. For Zn^{2+} titration experiments, increasing concentrations of $ZnCl_2$ were added to a solution containing WT peptide (25 μM) in 20 mM Tris-HCl, pH 7.5. CD spectra were recorded at each point of titration following 5 min of incubation after the addition of Zn^{2+}. The spectra were then corrected by subtraction of spectra obtained with buffer in the presence or absence of $ZnCl_2$. To determine the dissociation constant for the peptide-zinc interaction, the changes in molar ellipticity at a single wavelength were plotted against the total zinc ion concentration. The zinc ion concentration required for half-maximal change in ellipticity yielded the K_d value.

In DNA-binding experiments, increasing concentrations of various DNA substrates were added to a solution containing WT or mutant peptide (50 μM) in 20 mM Tris-HCl, pH 7.5, and 0.1 mM $ZnCl_2$. The spectra were recorded following 10 min of incubation after each addition of DNA. The spectra obtained for peptide·DNA complex were corrected by subtracting the spectra for DNA alone. The molar ellipticity (θ) values were obtained using the conversion factor of 100/*Cl*, where *C* is the peptide concentration (molar), and *l* is the path length (centimeters).

DNA Synapsis Assay—Reaction mixtures (20 μl) containing 20 mM Tris-HCl (pH 7.5), 0.1 mM $ZnCl_2$, and 10 pmol of indicated ^{32}P-labeled duplex DNA were incubated with Hop1 WT or mutant peptide at the indicated concentrations for 20 min at 30 °C. The reactions were terminated by the addition of proteinase K (0.2 mg/ml), SDS (0.2%), and KCl (0.1 M). Following incubation at 30 °C for 20 min, samples were loaded onto an 8% non-denaturing polyacrylamide gel and electrophoresed in 45 mM Tris borate buffer (pH 8.3) containing 10 mM KCl, 5 mM $MgCl_2$, and 1 mM EDTA at 10 V/cm at 24 °C for 4 h. The products were visualized by autoradiography.

Dimethyl Sulfate Interference Assay—Partial methylation of ^{32}P-labeled 48-bp duplex DNA containing a $(G/G)_8$ stretch was carried out with 0.1% dimethyl sulfate in TE buffer (10 mM Tris-HCl, pH 7.5, 1 mM EDTA) at 30 °C for 2 min (21, 22). The reaction was stopped by the addition of 50 μl of stop buffer (1.5 M sodium acetate, pH 7, 1 M 2-mercaptoethanol, and 25 μg of yeast tRNA/ml) and 300 μl of ethanol. DNA was precipitated with ethanol, followed by centrifugation at 14,000 rpm at 4 °C for 30 min. The pellet was washed with 70% ethanol, dried, and resuspended in TE buffer. A synapsis assay was carried out with partially methylated duplex DNA as described above. The duplex DNA and synapsis product were excised from the gel and eluted into TE buffer. DNA was precipitated with ethanol and subjected to cleavage by incubation with 1 M piperidine at 90 °C for 20 min. Samples were evaporated to dryness, and the pellets were resuspended in 90 μl of water. This procedure was repeated three times. The pellets were dissolved in a solution containing 80% formamide, 10 mM NaOH, and 0.1% each of bromphenol blue and xylene cyanol. Samples were dena-

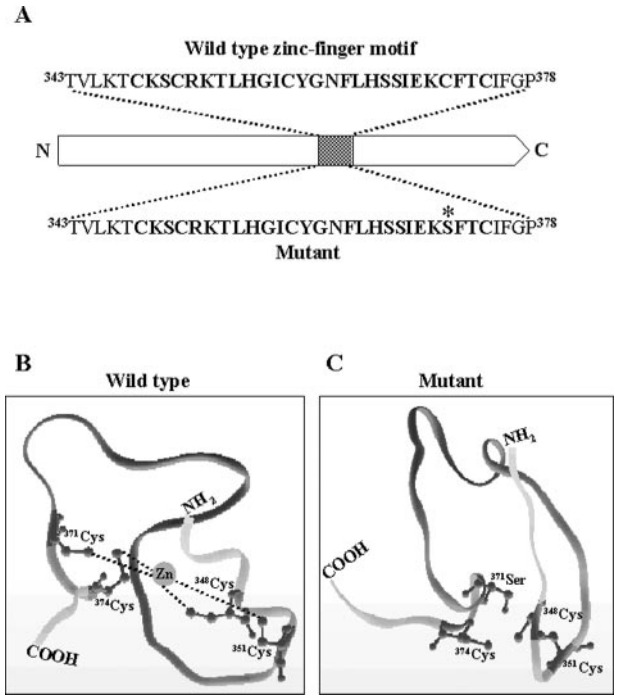

FIG. 1. *A*, sequences of wild type and mutant peptides corresponding to the Hop1 putative ZnF. The *open arrow* represents 605 amino acid residues of Hop1 protein from the amino-terminal (*N*) to carboxyl-terminal (*C*) ends. The *hatched region* corresponds to the putative ZnF. The figure uses the *single-letter* abbreviation to denote amino acids. *Highlighted* amino acids correspond to the putative ZnF. Five amino acids to the amino-terminal and four to the carboxyl-terminal ends were appended to the Hop1 ZnF to confer stability. *Asterisk* in the mutant peptide denotes change in sequence from Cys to Ser. *B*, theoretical model for the Hop1 ZnF generated by molecular threading. The cysteine residues are shown in coordination with a central zinc atom. *C*, theoretical model for the C371S mutant motif. Unlike the WT motif, C371S mutant apparently fails to fold into the classic U-shaped ZnF. The cysteine residues and S371 are depicted as *balls and sticks*.

tured at 100 °C for 10 min and kept on ice, and equal amounts of DNA (in terms of radioactivity) were loaded onto a 10% polyacrylamide gel containing 8 M urea. The gel was electrophoresed at 1800 V for 2 h, dried, and subjected to autoradiography. The bands were quantified in the UVItech gel documentation system, using UVI-BANDMAP software.

Modeling of the Zinc Finger Peptides—The Gene Threader Fold Recognition server (29) was used to search for folds with maximum similarity to the Hop1 putative ZnF. The best fold was used to thread the structure of peptides and visualized using the Biodesigner program (created by Piotr Rotkiewicz, 2001, version 0.7).

RESULTS

To explore the role of the ZnF motif in the mechanism of Hop1 function, we used four different approaches. First, the biochemical activity of WT ZnF in conjunction with its C371S mutant was assessed for their intrinsic affinity for zinc in zinc-binding assays. Second, these peptides were then examined for their ability to interact with DNA and promote pairing of DNA double helices. Third, interactions were substantiated using circular dichroism (CD) measurements by monitoring the conformational changes in the ZnF and filter-binding assays. Fourth, methylation interference experiments identified specific nucleotide residues involved in Hop1 ZnF promoted pairing of DNA double helices via the formation of G quartets.

Generation and Characterization of Hop1 ZnFs—To explore whether the putative Hop1 ZnF is biologically active, we generated two peptides (36-mer, residues 343–378): wild-type (WT) encompassing the putative ZnF and its corresponding C371S mutant (mutation is highlighted with an *asterisk*, Fig. 1A). A typical zinc finger is ~30 amino acid residues long and is folded into a compact domain with a carboxyl-terminal α-helix containing invariant Cys/His residues coordinated through zinc to the Cys/His of β-sheet at the amino-terminal end (30, 31). Although Hop1 ZnF is of similar length, its secondary structure differs from the previously characterized natural ZnFs. In particular, the positions of α-helix and β-sheet are inverted in the Hop1 ZnF (Fig. 1*B*). The schematic structure shows that the amino-terminal amino acids of Hop1 ZnF fold into the α-helical structure, whereas the residues at the carboxyl-terminal end fold into the β-sheet. As shown in Fig. 1*B*, a pair of cysteine residues reside in the α-helix, and an identical number in the β-sheet of the ZnF. Compared with the WT ZnF, its corresponding C371S mutant exhibits a substantially deviant secondary structure (Fig. 1*C*). The C371S mutant peptide formed a short α-helix, which appears to be inadequate to fold into the zinc-binding domain, suggesting that Cys^{371} plays a key role in contributing to the overall structural integrity of Hop1 protein. This is not surprising, because the energy associated with the coordination of zinc ion is known to facilitate folding of ZnFs (32, 33).

Zinc Binding by Hop1 ZnF—Because the Hop1 ZnF is shown to be essential for its function *in vivo* (13), the WT and its corresponding C371S mutant peptides were assessed for their ability to bind ^{65}Zn in zinc blot assays (34–36). The radioactive zinc blot assays have been used to demonstrate zinc-binding efficiencies to a variety of proteins and their mutants (37). Increasing concentrations of WT Hop1 ZnF and its corresponding C371S mutant were subjected to the zinc blot assay as described under "Materials and Methods." Briefly, increasing concentrations of the WT Hop1 ZnF and its corresponding C371S mutant were spotted on a strip of nitrocellulose paper. It was then incubated with ^{65}Zn, washed with excess buffer to remove the unbound ^{65}Zn, and subjected to autoradiography. The amount of ^{65}Zn bound to WT and mutant ZnF is shown in Fig. 2*A*. The results suggest that binding of ^{65}Zn by the WT ZnF is linear, whereas the C371S mutant ZnF bound increasing amounts of ^{65}Zn in the 2–10 μM range and then reach a plateau (Fig. 2*B*). However, it is not clear whether this represents a background activity of nonspecific zinc ion binding, or it possesses a weak but specific zinc-binding activity. The ZnFs often bind other divalent cations (38). The specificity of binding of ^{65}Zn to the Hop1 ZnFs was examined in the presence of nonradioactive Zn^{2+}, Cu^{2+}, Co^{2+}, Cd^{2+}, Ca^{2+}, Mg^{2+}, or Mn^{2+}. Whereas the binding activity was not affected by the presence of Ca^{2+}, Mg^{2+}, or Mn^{2+}, several metal ions that are capable of tetrahedral coordination decreased binding of ^{65}Zn to the WT Hop1 ZnF to varying extents (Fig. 2*C*).

Zinc Induces Conformational Changes in Hop1 ZnF—It is possible to assess metal ion binding to synthetic peptides by examining conformational changes in the secondary structure using circular dichroism (CD) spectroscopy in the far-UV region in the range of 175–260 nm (39). To ascertain whether the 36-mer peptides can fold into ZnFs, changes in their secondary structure were monitored in the absence or presence of increasing concentrations of Zn^{2+}. In the presence of Zn^{2+}, WT Hop1 ZnF displayed significant conformational changes in secondary structure, which led to the conversion of random coil to the ordered state (data not shown). The CD spectrum of the WT Hop1 ZnF·Zn^{2+} complex, compared with apo-ZnF, showed a change in negative molar ellipticity at 210 and 222 nm, characteristic of α-helix formation. These observations are reminiscent of zinc ion binding properties of synthetic or natural ZnFs of Rauscher murine leukemia virus nucleocapsid (40), *S. cerevisiae* transcriptional activator Adr1 (33), or *Xenopus laevis* TFIIIA (41). The change in ellipticity at 222 nm is plotted as a function of zinc ion concentration (Fig. 2*D*). CD data was sub-

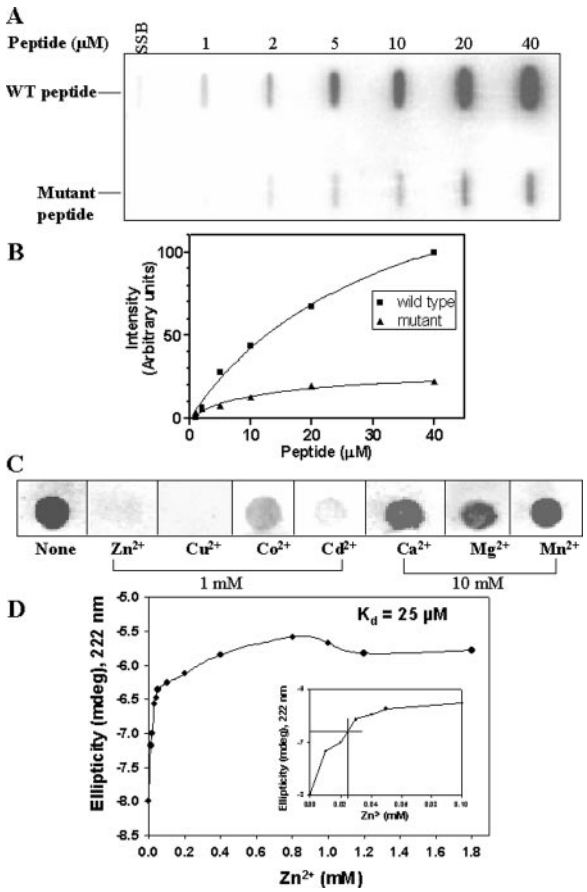

FIG. 2. **WT Hop1 ZnF displays high affinity while the C371S mutant reduced affinity for ^{65}Zn.** *A*, ^{65}Zn blot assay. Increasing concentrations of the WT or mutant peptide was blotted onto nitrocellulose membrane and probed with ^{65}Zn as described under "Materials and Methods." *E. coli* single-stranded DNA binding protein (*SSB*) was used as negative control. *B*, quantification of zinc binding. The autoradiogram shown in Fig. 2*A* was scanned, and the data are plotted against the peptide concentration. *C*, competition of ^{65}Zn binding by divalent metal ions. Wild type peptide (4 μg) was blotted onto nitrocellulose filter in multiple sets. Each strip was incubated with $^{65}ZnCl_2$ either in the absence (none) or presence of competitor metal ions at indicated concentrations. Blots were washed and visualized by autoradiography. *D*, determination of the dissociation constant of peptide·Zn^{2+} complex. The ellipticity values at 222 nm are plotted against the Zn^{2+} concentration. The K_d value was obtained from non-linear regression analysis.

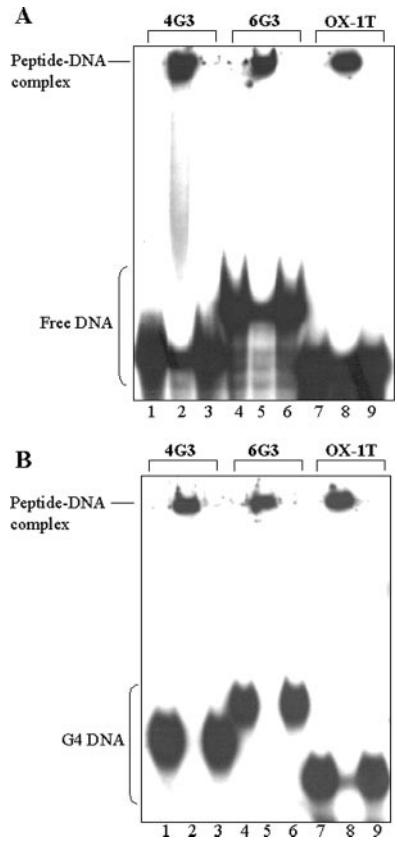

FIG. 3. **The Hop1 ZnF binds to G-rich oligonucleotides and G4 DNA.** *A*, binding of WT Hop1 ZnF and its corresponding C371S mutant to oligonucleotides containing arrays of G-rich residues (in their monomeric form). Reaction mixtures containing 20 mM Tris-HCl, pH 7.5, 0.1 mM $ZnCl_2$, and 10 pmol of specified ^{32}P-labeled oligonucleotide were incubated in the absence (*lanes 1*, *4*, and *7*) or presence of 5 μM WT Hop1 zinc finger (*lanes 2*, *5*, and *8*) or C371S mutant (*lanes 3*, *6*, and *9*) motif as described previously (21). *B*, binding of Hop1 WT or C371S mutant peptides to G4 DNA assembled from 4G3, 6G3, and OX-1T. 10 pmol of indicated ^{32}P-labeled G4 DNA was incubated in the absence (*lanes 1*, *4*, and *7*) or presence of 5 μM WT zinc finger (*lanes 2*, *5*, and *8*) or C371S mutant (*lanes 3*, *6*, and *9*) motif as described (21).

jected to non-linear regression analysis. The results yielded an apparent equilibrium dissociation constant (K_d) of 2.5×10^{-5} M. Together, these results suggest that WT Hop1 ZnF possesses metal-binding and structural characteristics of correctly folded ZnFs.

Hop1 ZnF Binds G4 DNA—We showed previously that full-length Hop1 displayed higher binding affinity for DNA rich in G residues and G4 DNA compared with normal DNA (21). The evidence that the WT Hop1 ZnF was able to bind Zn^{2+} and that the metal ion induced conformational changes in its secondary structure prompted us to investigate the possibility of whether Hop1 ZnF or its corresponding C371S mutant bind DNA. To explore this, we used 36-mer oligonucleotides bearing tracks of four (4G3) or six (6G3) guanine residues. Additionally, we used 39-mer oligonucleotide containing two tracks of four guanine residues (OX-1T). These were either in the monomeric form (Fig. 3*A*) or folded into G4 DNA (Fig. 3*B*) (21). Electrophoretic mobility shift assays were performed using various ^{32}P-labeled oligonucleotides containing increasing arrays of G residues. The assay conditions with regard to pH, temperature, and cofactor requirements were similar to those used for full-length Hop1 (21). The data in Fig. 3*A* (*lanes 2*, *5*, and *8*) show that the wild type Hop1 ZnF was able to bind labeled DNA in a manner similar to that of the full-length Hop1 protein (21). In contrast, the same assay revealed no evidence for binding of the C371S mutant ZnF to DNA (Fig. 3*A*, *lanes 3*, *6*, and *9*). The results obtained by this assay are specific, because a similar behavior was also evident with three different DNA substrates and that the C371S mutant ZnF failed to form detectable nucleoprotein complexes. These data allow us to conclude that the putative ZnF of Hop1 constitutes the minimal DNA-binding domain. Having demonstrated a direct interaction between oligonucleotide substrates and Hop1 ZnF, we investigated whether it can bind G4 DNA, a substrate previously shown to be specific for Hop1 protein (21). We used the same 36-mer substrates that do not share much homology with each other but as shown previously (21), can form G4 DNA. As shown in Fig. 3*B*, the WT Hop1 ZnF displayed avid binding to G4 DNA, whereas the C371S mutant peptide did not. In parallel experiments, we observed that WT Hop1 ZnF, but not C371S mutant peptide, was able to bind various topological forms of bacteriophage M13 DNA (data not shown). Together, these results suggest that C371S mutant ZnF is broadly defective in DNA-binding activity.

Hop1 ZnF Promotes the Formation of G4 DNA—We next investigated the ability of Hop1 ZnF and its corresponding C371S mutant to promote the formation of G4 DNA. Varying

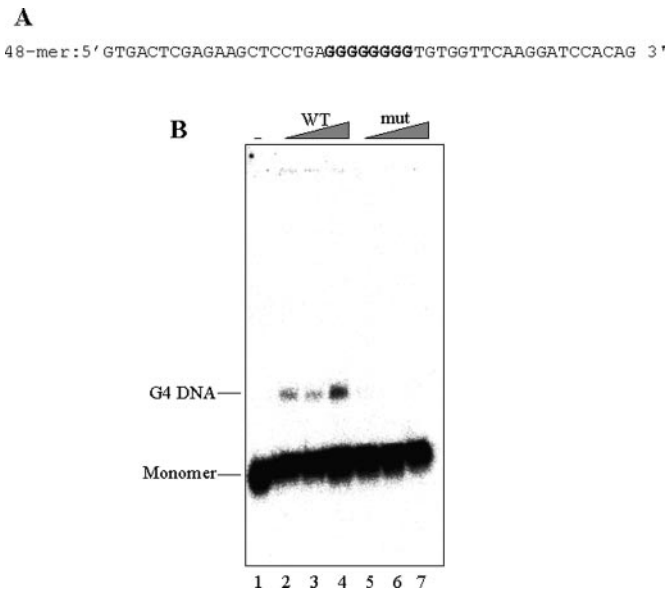

FIG. 4. **Hop1 ZnF promotes the formation of G4 DNA.** *A*, sequence of the oligonucleotide used. *Highlighted letters* indicate the array of eight G residues. *B*, WT Hop1 ZnF and not its C371S mutant promote the formation of G4 DNA. Increasing concentrations of the WT Hop1 or C371S mutant motif was incubated with 10 pmol of ^{32}P-labeled oligonucleotide and analyzed for G4 DNA formation as described (21). *Lanes 1–7*, DNA incubated in the absence (*lane 1*) or presence of 1, 2.5, or 5 μM of WT (*lanes 2–4*) or C371S mutant (*lanes 5–7*) peptide, respectively. The position of monomer and G4 DNA is indicated on the *left*.

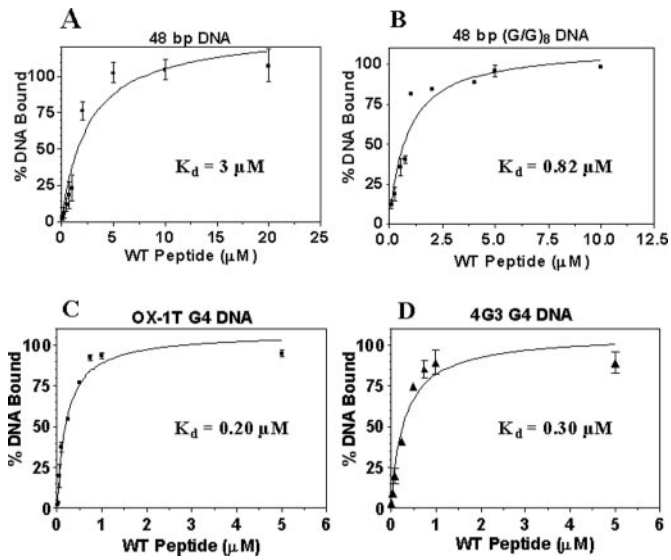

FIG. 5. **Filter binding assay to determine the affinity of Hop1 ZnF to various types of DNA.** The indicated concentrations of Hop1 ZnF was incubated with 10 pmol of ^{32}P-labeled duplex or G4 DNA and analyzed as described under "Materials and Methods." The percentage of DNA bound to ZnF is plotted against the added amount of the peptide. The figure shows the data obtained for the 48-bp duplex DNA of mixed base sequence (*panel A*), 48-bp duplex DNA containing mismatched 8-bp G/G sequence embedded at the center (*panel B*), and G4 DNA assembled from OX-1T (*panel C*) or 4G3 (*panel D*). Non-linear regression analysis of the data yielded the K_d for various substrates, which are depicted in the *inset*. The data in each panel represent an average of two independent determinations.

concentrations of WT Hop1 ZnF or its corresponding C371S mutant were incubated with oligonucleotide containing a stretch of eight G residues (Fig. 4*A*). Subsequently, the peptides were removed by incubation with proteinase K (22). Samples were separated by gel electrophoresis under non-denaturing conditions and visualized by autoradiography (22). As shown in Fig. 4*B*, the WT Hop1 ZnF was able to promote the formation of G4 DNA, whereas its C371S mutant at the same concentration range did not. The correlation between binding of Hop1 ZnF to G4 DNA and the formation of G4 DNA reinforces the notion that Hop1 ZnF is sufficient for the display of all of the known activities of full-length Hop1 under *in vitro* conditions.

Hop1 ZnF Displays Higher Affinity for G4 DNA—To explore the apparent affinity of Hop1 ZnFs for DNA, we used two types of duplex substrates: 48-bp B-form DNA, an identical DNA fragment containing a mismatched 8-bp G/G sequence embedded at the center, and G4 DNA. The relative affinity of Hop1 ZnF to these DNA substrates was determined using a nitrocellulose filter-binding assay. The ^{32}P-labeled DNA substrates were incubated with increasing concentrations of WT Hop1 ZnF and assayed as described under "Materials and Methods." Comparison of data revealed that lesser amounts of Hop1 ZnF were required to achieve the formation of maximum amounts of nucleoprotein complexes with G4 DNA compared with B-form DNA (Fig. 5). The filter-binding assay yielded a binding stoichiometric ratio of 3 bp/Hop1 peptide. The apparent K_d values were calculated by non-linear regression method, assuming that the Hop1 peptide is 100% active and interacts with DNA as a monomer. The K_d values (in the micromolar range) for interaction of WT Hop1 ZnF with various duplex DNA substrates were similar, although it displayed ~15-fold higher affinity for G4 DNA over B-form DNA (Fig. 5, *inset*). Moreover, the presence of a mismatched 8-bp G/G sequence in an otherwise identical duplex DNA led to an increase in the affinity by 3- to 4-fold (Fig. 5, compare *A* to *B*). We believe that the data are not an artifact of the filter-binding assay, because this assay has been used in numerous instances to determine the binding efficiencies of full-length as well as synthetic ZnFs to nucleic acid substrates (42). In addition, the binding constants obtained are comparable to those reported for the full-length Hop1 protein (21, 28). However, it is interesting to note that the ZnF, like the full-length Hop1, can readily distinguish B-form DNA from that of G4 DNA. Furthermore, like in the case of full-length Hop1, binding of the Hop1 ZnF to ^{32}P-labeled duplex DNA is sensitive to preincubation with increasing concentrations of NaCl (Fig. 6).

DNA Induces Conformational Changes in the Hop1 ZnF—We reasoned that if WT Hop1 peptide functions as a canonical ZnF, then its interaction with DNA might induce conformational changes (43). Conversely, similar changes may not be apparent in the C371S mutant peptide. We tested this possibility by monitoring conformational changes in apo-peptides upon interaction with DNA. To examine ligand-induced changes in the apo-peptides, we used double-stranded DNA, because full-length Hop1 displayed vastly enhanced binding affinity for duplex DNA over ssDNA. The spectra of WT peptide showed a substantial decrease in negative molar ellipticity at 210 and 222 nm in the presence of DNA (Fig. 7*A*). No changes in the spectrum were apparent at 245 nm or with increasing concentration of DNA (above 2 μM). By contrast, the C371S mutant peptide failed to display similar changes, thereby precluding a similar interaction with double-stranded DNA (Fig. 7*B*). Together, these results indicate that the Hop1 $^{348}CX_2CX_{19}CX_2C^{374}$ sequence motif is indeed a functional ZnF.

Hop1 ZnF Promotes Synapsis between Two DNA Double Helices—The characterization of Hop1 ZnF made it possible to test its biochemical activity using a functional assay that has been developed for Hop1 protein (22). In particular, we chose to investigate whether ZnF can promote synapsis between two DNA double helices. In one set of experiments, increasing concentrations of WT ZnF or its corresponding C371S mutant was incubated with ^{32}P-labeled 48-bp duplex DNA containing a

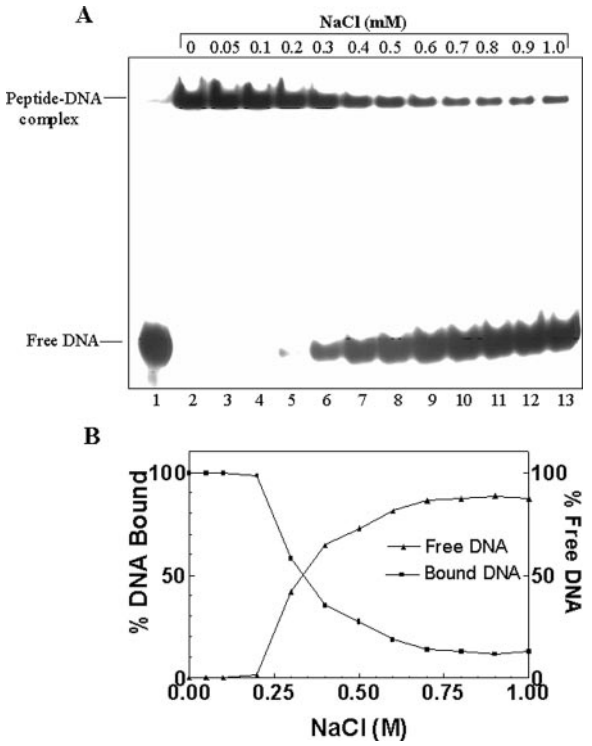

FIG. 6. **Salt affects the binding of Hop1 ZnF to duplex DNA.** *A*, reactions were performed with the concentrations of NaCl as indicated *above each lane*. The ^{32}P-labeled 48-bp duplex DNA containing 8-bp mismatched G/G sequence was incubated in the absence (*lane 1*) or presence of 5 μM Hop1 ZnF (*lanes 2–13*). *B*, quantification of peptide·DNA complexes. The autoradiogram shown in *A* was densitometrically scanned, and the data shown are the percentage of DNA bound (■) and free DNA (▲) against NaCl concentration.

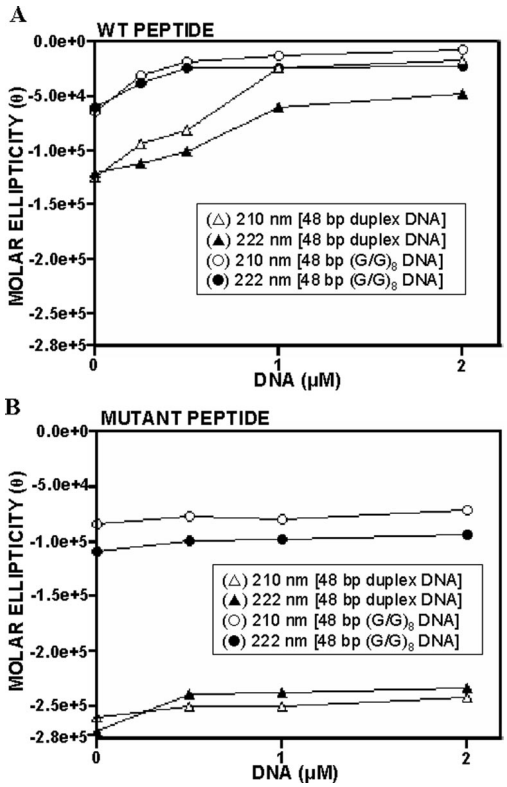

FIG. 7. **Hop1 ZnF displays DNA-induced conformational changes.** The decline in negative molar ellipticity (θ) of the WT Hop1 ZnF (*A*) and its corresponding C371S mutant (*B*) at 210 and 222 nm is plotted against DNA concentration.

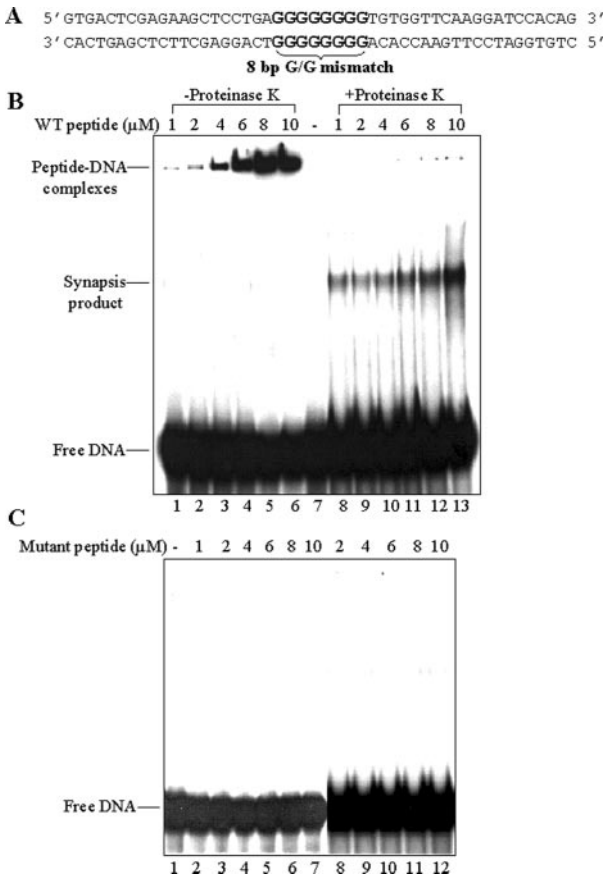

FIG. 8. **Hop1 ZnF promotes synapsis between DNA double helices containing mismatched G/G sequences.** *A*, schematic of the DNA substrate. *Highlighted* bases indicate the mismatched G/G sequences. *B*, WT peptide promotes synapsis of DNA double helices containing a mismatched 8-bp G/G sequence. Ten picomoles of ^{32}P-labeled duplex DNA was incubated in the absence (*lane 7*) or presence of WT Hop1 ZnF at concentrations indicated at the *top of each lane*. One set of samples was assayed for DNA binding (*lanes 1–6*), whereas the second set of samples was assayed for the formation of synapsis product (*lanes 8–13*). *C*, the C371S hop1 mutant peptide failed to bind DNA and defective in promoting synapsis of DNA double helices. Ten picomoles of ^{32}P-labeled duplex DNA was incubated in the absence (*lane 1*) or presence of C371S mutant peptide at concentrations indicated above each lane. One set of samples was assayed for DNA binding (*lanes 2–7*), whereas the second set was analyzed for synapsis product formation (*lanes 8–12*).

centrally embedded 8-bp mismatched G/G region (Fig. 8*A*). In parallel, reactions were performed in a similar manner, but prior to electrophoresis the samples were deproteinized by incubation with proteinase K as described under "Materials and Methods." As shown in Fig. 8*B* (*lanes 1–6*), ZnF was able to form a distinct peptide·DNA complex in a concentration-dependent manner. Most strikingly, ZnF was able to promote synapsis of DNA double helices (Fig. 8*B*, *lanes 8–13*), a feature reminiscent of that of the full-length Hop1 protein (22). Quantification of product suggested that the extent of synapsis was ~35% in the presence of 10 μM ZnF (Fig. 8*B*, *lane 13*). The formation of synapsis product was in the same concentration range as full-length Hop1, and a further increase in the concentration of ZnF failed to increase the extent of synapsis product formation (data not shown). In contrast to this, the C371S mutant peptide failed to interact with DNA (Fig. 8*C*, *lanes 2–7*), and as a result was unable to promote synapsis product formation (Fig. 8*C*, *lanes 8–12*).

To extend our observations, we examined the ability of Hop1 ZnF to promote the formation of synapsis product with various mutant DNA substrates (Fig. 9*A*). As observed for the full-

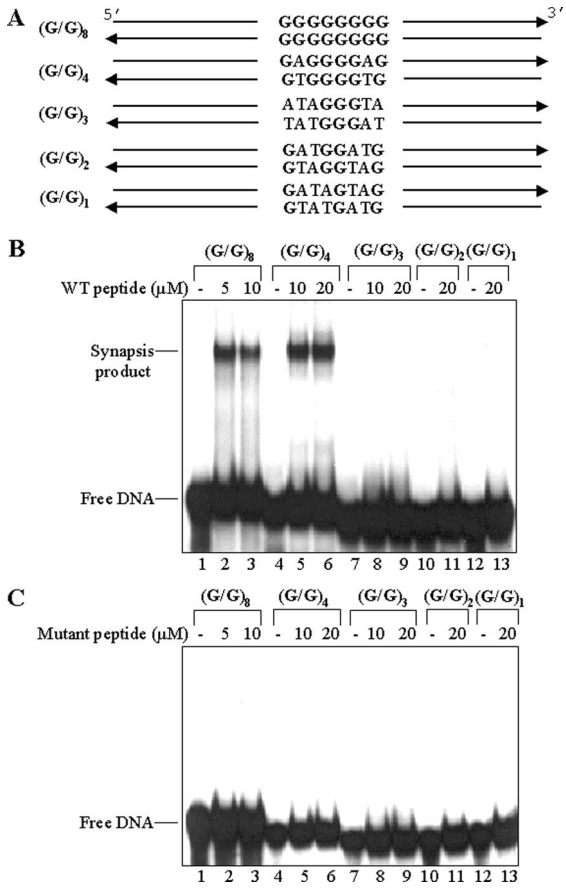

FIG. 9. **Mutations in the G/G region diminish synapsis between double-stranded DNA helices.** *A*, schematic of the DNA substrates. The mismatched G/G bp is shown in *boldface*. *B*, Hop1 zinc-finger promoted synapsis of DNA bearing mutation in the G/G region. 10 pmol each of the indicated ^{32}P-labeled duplex DNA was incubated with Hop1 ZnF at concentrations as shown above each lane for 20 min at 30 °C. The reactions were deproteinized and analyzed as described under "Materials and Methods." The subscript to *G/G parenthesis* denotes the number of contiguous mismatched G/G bp. *C*, the C371S hop1 mutant fails to promote synapsis of 48-bp duplex DNA substrates containing varying number of G/G bp. Reactions were performed as described for *B*.

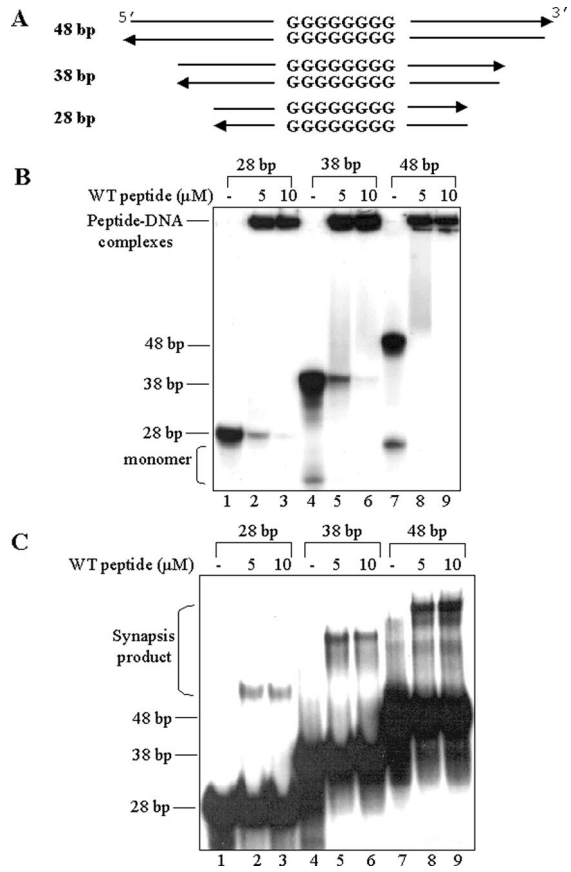

FIG. 10. **Minimum sequence required for WT Hop1 ZnF to promote synapsis between two double-stranded DNA helices.** *A*, schematic of the DNA substrates. *B*, WT Hop1 ZnF binds to shorter DNA substrates. Reactions mixtures contained 10 pmol of ^{32}P-labeled duplex DNA and WT Hop1 ZnF at concentrations as indicated *above each lane*. Samples were incubated at 30 °C for 20 min and analyzed as described under "Materials and Methods." *C*, WT Hop1 ZnF promotes synapsis between DNA of varying length. Reactions were performed as described for *B*. Samples were deproteinized and analyzed as described under "Materials and Methods." The position of each of the duplex DNA and their synapsis product is indicated on the *left*.

length Hop1 protein (22), control experiments showed that WT ZnF promoted a robust synapsis of the duplex DNA substrate containing an 8-bp mismatched region (Fig. 9*B*, *lanes 2* and *3*). Furthermore, substitution of a pair of G/G bp for A/T bp led to marginal decrease in the extent of synapsis, relative to the "WT" substrate (Fig. 9*B*, *lanes 5* and *6*). However, when three and two G/G mismatches from each end flanking the central 3-bp G/G array was replaced, synapsis was completely abolished (Fig. 9*B*, *lanes 8* and *9*). Notably, ZnF failed to display synapsis with substrates containing either two contiguous or three non-contiguous mismatched G/G bp (Fig. 9*B*, *lanes 10–13*). These results suggest that a minimum of four contiguous G residues, alone, are essential and sufficient for synapsis promoted by ZnF. Importantly, under similar conditions, the C371S ZnF failed to promote synapsis with the mutant DNA substrates (Fig. 9*C*). In additional experiments, we ascertained that the defect in synapsis product formation emanated from the inability of C371S mutant to interact with DNA (data not shown). These results suggest that ZnF, like the full-length Hop1 (22), was able to distinguish the base sequence in the pairing DNA double helices.

ZnF Promotes Synapsis between Shorter DNA Substrates—Previously, we showed that the binding stoichiometric ratio of full-length Hop1 protein to duplex DNA is ~50 bp/monomer of Hop1 (28). While characterizing the DNA-binding properties of Hop1 ZnF to duplex DNA using the filter-binding assay, we observed a binding stoichiometric ratio in the range of 3 bp/1 ZnF (data not shown). This observation raised the possibility of whether Hop1 ZnF can bind and promote synapsis between shorter DNA substrates (Fig. 10*A*). By comparison with full-length Hop1 (22, 28), the results shown in Fig. 10*B* suggest that Hop1 ZnF was able to form a stable DNA·peptide complex with DNA substrates ranging in length from 28 to 48 bp. To determine whether the binding of Hop1 ZnF to 28- or 38-bp fragments had led to the formation of synapsis product, samples were deproteinized, separated by polyacrylamide gel electrophoresis, and visualized by autoradiography. The results shown in Fig. 10*C* suggest that Hop1 ZnF was able to generate synapsis product consistent with the formation of peptide·DNA complex. However, the amount of synapsis product formation with 28- and 38-bp fragments is less efficient compared with the 48-bp fragment.

Synapsis between DNA Double Helices Promoted by Hop1 ZnF Involve Formation of G4 DNA—Methylation interference is a sensitive method to identify the guanine residues important for the formation of G4 DNA (22, 44). To examine whether synapsis occurs via the formation of G4 DNA, the ^{32}P-labeled 48-bp mismatched G/G DNA was incubated with indicated concentrations of Hop1 ZnF. After deproteinization, each of the products was isolated from the gel, and its methylation pattern

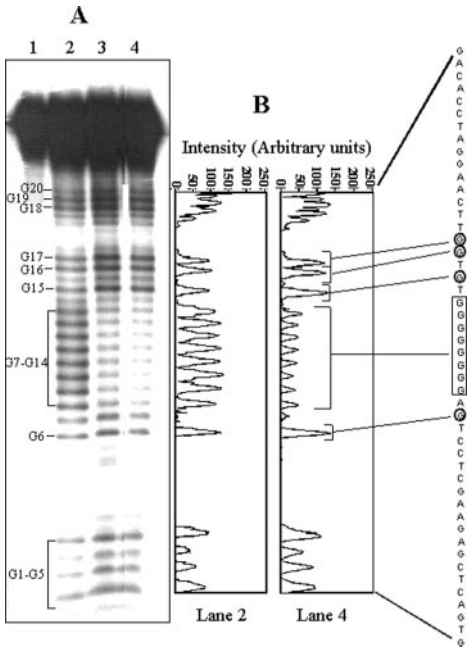

FIG. 11. **Methylation interference assay reveals the formation of guanine quartets during synapsis promoted by the WT Hop1 ZnF.** *A*, methylation pattern of the guanine residues in the 48-bp $(G/G)_8$ duplex DNA and the synapsis product. Reactions were performed as described under "Materials and Methods." *Lane 1*, 48-bp $(G/G)_8$ duplex DNA control; *2*, methylation pattern of 48-bp $(G/G)_8$ duplex DNA; *3* and *4*, methylation pattern of synapsis product generated in the presence of 5 and 10 μM WT Hop1 ZnF, respectively. *B*, quantitative scan of the autoradiogram shown in *A*, depicting the intensities of guanine residues in duplex DNA (*lane 2*) and synapsis product (*lane 4*). The protected guanine residues spanning the $(G/G)_8$ region are *boxed*, whereas those in the flanking region are *circled*.

was analyzed. Fig. 11*A* (*lane 2*) shows that in the absence of Hop1 ZnF, all guanines were methylated to a similar extent, suggesting that N7 guanine is accessible for methylation. In contrast, a direct correlation was observed between the concentration of ZnF and the extent of protection: with increasing concentrations of ZnF the guanines in the array, but not the flanking region, showed relatively greater protection against methylation. The guanine residues (G7–G14) at the center of the 8-bp G/G region had become increasingly resistant to methylation (Fig. 11, *lane 3* and *4*). The tracing of the autoradiogram indicated ~3-fold protection in the mismatched G/G region, compared with the reaction performed in the absence of Hop1 ZnF (Fig. 11*B*). These results suggest that the guanine residues in the mismatched G/G region are involved in interstitial synapsis of double-stranded DNA helices via the formation of guanine quartets.

DISCUSSION

In this study, we show that a 36-mer synthetic peptide encompassing the Hop1 putative ZnF ($^{348}CX_2CX_{19}CX_2C^{374}$) performs all of the known biochemical functions of full-length Hop1 protein. To elucidate the nature and function of Hop1 ZnF, interaction between peptides and metal ions were examined. We observed that the motif was able to bind zinc and, as a consequence, caused significant decrease in negative ellipticity, indicating conformational changes in its secondary structure. In contrast, such changes were not detectable in the C371S mutant peptide, suggesting direct involvement of Cys^{371} in zinc binding. Although only crystal structure can define the details of secondary structure, theoretical considerations predict that Hop1 ZnF is an atypical ZnF and differs from those in TFIIIA-like DNA-binding proteins (30). Competition experiments showed that a subset of divalent metal ions that are capable of tetrahedral coordination were able to compete with zinc for binding to the Hop1 ZnF. Together, these results suggest that Hop1 ZnF functions as an independent zinc-binding module.

The one or more biochemical roles for any of the SC proteins are not known, simply because samples of pure protein and/or assays have not been developed. These results are consistent with a biochemical role of Hop1 as a DNA-binding protein in interstitial pairing of meiotic chromosomes. We also showed that binding of Hop1 to DNA was sequence-independent but structure-specific (21). In the present study, we show that Hop1 ZnF plays a dual role: robust binding to G4 DNA and catalyst for the folding of DNA into this conformation; therefore, this represents a novel type of ZnF.

How can we reconcile the observation that Hop1 ZnF alone is sufficient for the display of all of the known activities of full-length Hop1 protein? What would be the function of the remaining part of Hop1 protein? One of the answers to this question lies in the fact that the different domains might be involved in its interaction with other SC components. In this regard, Hop1 has been shown to interact genetically with *RED1* and forms a complex with its gene product (20, 45, 46). However, the domains involved in interaction between Hop1 and Red1 proteins remain to be identified. In furthering our understanding of the mechanism of Hop1 function, a combination of structural analysis and functional characterization of interaction between ZnF and ^{65}Zn on one hand, and DNA and ZnF on the other, has been particularly informative. Structural characterization of the binding of ^{65}Zn to ZnF and its interaction with DNA has not only revealed the physical basis for the defect of C371S *hop1* mutant allele *in vivo* but also allowed the identification of novel type of zinc finger.

To investigate the biochemical function of Hop1 ZnF, we studied its binding to various DNA substrates. We used gel mobility shift assays in combination with methylation interference to demonstrate binding of Hop1 to DNA rich in arrays of G residues as well as the formation of G4 DNA. Hop1 ZnF, like the full-length protein, preferentially binds to DNA-containing arrays of G residues and G4 DNA, and it promotes the formation of the latter. In contrast, the C371S mutant is impaired in both ^{65}Zn-binding and DNA-binding properties, indicating that the integrity of ZnF is very important for Hop1 function *in vivo*. Remarkably, interaction of Hop1 ZnF with different DNA substrates was functionally indistinguishable from that of the full-length Hop1 protein (21, 22, 28 and this study). However, ZnF but not the full-length Hop1 bound shorter DNA fragments and promoted synapsis product formation. The observation that Hop1 ZnF displayed all of the activities of full-length Hop1 is analogous to that of *Escherichia coli* RecA. In particular, a 20-mer peptide of RecA was able to promote both ATPase and strand exchange activities (47). It is likely that these are biologically relevant, because the same properties and kinetics were also evident with the full-length Hop1 protein (21, 22, 28).

Numerous ZnFs have been characterized from a variety of proteins and sources. Although some are thought to function through binding to nucleic acids, a subset of them has been implicated in protein-protein interaction (23, 48). ZnFs often prefer G-rich sequences in DNA operators and bind through major groove (49). Each of them recognizes a DNA base triplet in its respective binding site (50). An engineered modular ZnF has been shown to bind oligonucleotides containing the human telomeric repeat sequence folded into G4 DNA (51). Several G4 DNA-binding proteins have been isolated from a variety of sources, which display high affinity for DNA sequences (52, 53). The affinity of Hop1 ZnF to DNA (micromolar range) is com-

parable to those reported for other known ZnFs. Most of these have been shown to possess moderate binding affinities and discriminate weakly between duplex and quadruplex DNA (54). Similarly, naturally occurring high affinity telomere-binding proteins are also unable to discriminate these structures. For example, *S. cerevisiae* RAP1 has distinct but inseparable domains for binding G4 DNA and double-stranded DNA (55). However, there is no evidence to show that the ZnF can promote synapsis between two DNA double helices or formation of G4 DNA.

To our knowledge, Hop1 ZnF is the first example of a ZnF that has been shown to promote synapsis between DNA double helices. The existence of intracellular G quadruplexes in ciliates (56) and G quadruplex-forming sequences in the telomeres suggests that G4 DNA may facilitate proper alignment of homologous chromosomes during meiosis (44, 57, 58) and may be important to the mechanism and regulation of telomere extension (59, 60). Accordingly, several lines of evidence indicate that clustering of telomeres is required for meiotic chromosome pairing and recombination (61, 62). Although a great deal is yet to be learned about the mechanism of Hop1 protein function in meiotic chromosome pairing and synapsis, our biochemical evidence suggest that Hop1 ZnF might play a crucial role in these processes.

Acknowledgment—We thank Ms. Gitanjali Yadav for her assistance in modeling Hop1 zinc finger motifs.

REFERENCES

1. Scherthan, H., Loidl, J., Schuster, T., and Schweizer, D. (1992) *Chromosoma* **101,** 590–595
2. Hiraoka, Y. (1998) *Genes Cells* **3,** 405–413
3. von Wettstein, D., Rasmussen, S. W., and Holm, P. B. (1984) *Annu. Rev. Genet.* **18,** 331–413
4. Kleckner, N., and Weiner, B. M. (1993) *Cold Spring Harbor. Symp. Quant. Biol.* **58,** 553–565
5. Zickler, D., and Kleckner, N. (1998) *Annu. Rev. Genet.* **32,** 619–697
6. Sym, M., and Roeder, G. S. (1994) *Cell* **79,** 283–292
7. Roeder, G. S. (1997) *Genes Dev.* **11,** 2600–2621
8. Zickler, D., and Kleckner, N. (1999) *Annu. Rev. Genet.* **33,** 603–754
9. Loidl, J., Klein, F., and Scherthan, H. (1994) *J. Cell Biol.* **125,** 1191–1200
10. Weiner, B. M., and Kleckner, N. (1994) *Cell* **77,** 977–991
11. Nag, D. K., Scherthan, H., Rockmill, B., Bhargava, J., and Roeder, G. S. (1995) *Genetics*, **141,** 75–86
12. Hollingsworth, N. M., and Byers, B. (1989) *Genetics* **121,** 445–462
13. Hollingsworth, N. M., Goetsch, L., and Byers, B. (1990) *Cell* **61,** 73–84
14. Rockmill, B., and Roeder, G. S. (1988) *Proc. Natl. Acad. Sci. U. S. A.* **85,** 6057–6061
15. Sym, M., and Roeder, G. S. (1995) *J. Cell Biol.* **128,** 455–466
16. Sym, M., Engebrecht, J., and Roeder, G. S. (1993) *Cell* **72,** 365–378
17. Chua, P. R., and Roeder, G. S. (1998) *Cell* **93,** 349–359
18. Agarwal, S., and Roeder, G. S. (2000) *Cell* **102,** 245–255
19. Leu, J.-Y., Chua, P. R., and Roeder, G. S. (1998) *Cell* **94,** 375–386
20. Smith, A. V., and Roeder, G. S. (1997) *J. Cell Biol.* **136,** 957–967
21. Muniyappa, K., Anuradha, S., and Byers, B. (2000) *Mol. Cell. Biol.* **20,** 1361–1369
22. Anuradha, S., and Muniyappa, K. (2004) *Nucleic Acids Res.* **32,** 2378–2385
23. Laity, J. H., Lee, B. M., and Wright, P. E. (2001) *Curr. Opin. Struct. Biol.* **11,** 39–46
24. Freidman, D. B., Hollingsworth, N. M., and Byers, B. (1994) *Genetics* **136,** 449–464
25. Johnston, M., and Dover, J. (1987) *Proc. Natl. Acad. Sci. U. S. A.* **84,** 2401–2405
26. Sambrook, J., Fritsch, E. F., and Maniatis, T. (1989) *Molecular Cloning: A Laboratory Manual*, 2nd Ed., Cold Spring Harbor Laboratory Press, New York
27. Cunningham, R. P., Dasgupta, C., Shibata, T., and Radding, C. M. (1980) *Cell* **20,** 223–225
28. Kironmai, K. M., Muniyappa, K., Friedman, D., Hollingsworth, N. M., and Byers, B. (1998) *Mol. Cell. Biol.* **18,** 1424–1435
29. Jones, D. T. (1999) *J. Mol. Biol.* **287,** 797–815
30. Lee, M. S., Gippert, G. P., Soman, K. V., Case, D. A., and Wright, P. E. (1989) *Science* **245,** 635–637
31. Klevit, R. E., Herriot, J. R., and Horvath, S. J. (1990) *Proteins* **7,** 215–226
32. Pan, T., and Coleman, J. E. (1990) *Proc. Natl. Acad. Sci. U. S. A.* **87,** 2077–2081
33. Parraga, G., Horvath, S. J., Eisen, A., Taylor, W. E., Hood, L., Young, E. T., and Klevit, R. E. (1988) *Science* **241,** 1489–1492
34. Schiff, L. A., Nibert, M. L., and Fields, B. N. (1988) *Proc. Natl. Acad. Sci. U. S. A.* **85,** 4195–4199
35. Treich, I., Riva, M., and Sentenac, A. (1991) *J. Biol. Chem.* **266,** 21971–21976
36. Bestor, T. H. (1992) *EMBO J.* **11,** 2611–2617
37. Donalson, I. M., and Friesen, J. D. (2000) *J. Biol. Chem.* **275,** 13780–13788
38. Vallee, B. L., and Galdes, A. (1984) *Adv. Enzymol.* **56,** 283–431
39. Johnson, C. W., Jr. (1990) *Proteins: Struct. Funct. Genet.* **7,** 205–214
40. Green, L. M., and Berg, J. M. (1989) *Proc. Natl. Acad. Sci. U. S. A.* **86,** 4047–4051
41. Frankel, A. D., Berg, J. M., and Pabo, C. O. (1987) *Proc. Natl. Acad. Sci. U. S. A.* **84,** 4841–4845
42. Archer, T. K., Hager, G. L., and Omichinski, J. G. (1990) *Proc. Natl. Acad. Sci. U. S. A.* **87,** 7560–7564
43. Andrade, M. A., Chacón, P., Merelo, J. J., and Morán, F. (1993) *Prot. Eng.* **6,** 383–390
44. Sen, D., and Gilbert, W. (1988) *Nature* **334**, 364–366
45. de los Santos, T., and Hollingsworth, N. M. (1999) *J. Biol. Chem.* **274,** 1783–1790
46. Hollingsworth, N. M., and Ponte, L. (1997) *Genetics* **147,** 33–42
47. Voloshin, O. N., Lijiang, W., and Camerini-Otero, R. D. (1996) *Science* **272,** 868–872
48. Cook, C. R., Kung, G., Peterson, F. C., Volkman, B. F., and Lei, M. (2003) *J. Biol. Chem.* **278,** 36051–36058
49. Jamieson, A. C., Wang, H., and Kim, S. H. (1996) *Proc. Natl. Acad. Sci. U. S. A.* **93,** 12834–12839
50. Pavletich, N. P., and Pabo, C. O. (1991) *Science* **252,** 809–817
51. Isalan, M., Patel, S. D., Balasubramanian, S., and Choo, Y. (2001) *Biochemistry* **40,** 830–836
52. Arthanari, H., and Bolton, P. H. (2001) *Chem. Biol.* **8,** 221–230
53. Shafer, R. H., and Smirnov, I. (2001) *Biopolymers* **56,** 209–227
54. Brown, B. A., Li, Y., Brown, J. C., Hardin, C. C., Roberts, J. F., Pelsue, S. C., and Shultz, L. D. (1998) *Biochemistry* **37,** 16325–16337
55. Giraldo, R., Suzuki, M., Chapman, L., and Rhodes, D. (1994) *Proc. Natl. Acad. Sci. U. S. A.* **91,** 7658–7662
56. Schaffitzel, C., Berger, I., Postberg, J., Hanes, J., Lipps, H. J., and Pluckthun, A. (2001) *Proc. Natl. Acad. Sci. U. S. A.* **98,** 8572–8577
57. Sundquist, W. L., and Klug, A. (1989) *Nature* **342,** 825–829
58. Williamson, J. R., Raghuraman, M. K., and Cech, T. R. (1989) *Cell* **59,** 871–880
59. Salazar, M., Thompson, B. D., Kerwin, S. M., and Hurley, L. H. (1996) *Biochemistry* **35,** 16110–16115
60. Sun, D., LopezGuajardo, C. C., Quada, J., Hurley, L. H., and VonHoff, D. D. (1999) *Biochemistry* **38,** 4037–4044
61. Scherthan, H., Weich, S., Schwegler, H., Heyting, C., Härle, M., and Cremer, T. (1996) *J. Cell Biol.* **134,** 1109–1125
62. Rockmill, B., and Roeder, G. S. (1998) *Genes Dev.* **12,** 2574–2586